



## Red dye 40 removal by fixed-bed columns packed with alginate-chitosan sulfate hydrogels

### Remoción del colorante rojo 40 por medio de columnas de lecho fijo empacadas con hidrogeles de alginato-sulfato de quitosano

I.P. Verduzco-Navarro<sup>1</sup>, C.F. Jasso-Gastinel<sup>2</sup>, N. Rios-Donato<sup>1</sup>, E. Mendizábal<sup>1\*</sup>

<sup>1</sup>Departamento de Química, CUCEI, Universidad de Guadalajara, Jalisco, 44430, México.

<sup>2</sup>Departamento de Ingeniería Química, CUCEI, Universidad de Guadalajara, Jalisco, 44430, México.

Received: December 28, 2019; Accepted: February 24, 2020

#### Abstract

Modified Chitosan was used for the removal of red dye 40 from aqueous solutions at a pH of 5.0. The adsorption was carried in fixed-bed columns packed with beads of Alginate-Chitosan Sulfate (Alg-ChS) hydrogels. Two columns of 13 and 33 cm of height and two feed rates (20 and 40 mL/h) were used. The pH of the dye solutions at the exit of the columns was much higher than the one registered at the entrance which can be explained by protons transfer from the aqueous solution to the amino and hydroxyl groups of the Alg-ChS and to the carboxylate groups of the alginate. The increase in pH favored the removal of the dye. The breakthrough time and the amount of dye removed decreased when the flow rate was increased. Greater dye removal was achieved when the higher column was used. After the breakthrough time, the columns continued to remove appreciable amounts of dye and even after 50 hours of operation, the columns did not reach saturation.

**Keywords:** chitosan sulfate, alginate, fixed-bed column, pH increase, Red Dye 40.

#### Resumen

Se utilizó quitosano modificado para la remoción del colorante rojo 40 de soluciones acuosas con un pH de 5.0. La adsorción se llevó a cabo utilizando dos columnas de lecho fijo rellenas con perlas de hidrogeles de Alginato-Sulfato de Quitosano (Alg-ChS). Se utilizaron dos columnas con alturas de 13 y 33 cm, y dos velocidades de alimentación (20 y 40 mL/h). El pH de las soluciones de colorante a la salida de las columnas era mucho más alto que el de la entrada, lo que puede explicarse por la transferencia de protones desde la solución acuosa a los grupos amino e hidroxilo del Alg-ChS y a los grupos carboxilato del alginato. El aumento del pH fue favorable para la remoción del colorante. El tiempo de ruptura y la cantidad de colorante eliminado disminuyeron cuando se incrementó el flujo. Se logró una mayor remoción de colorante cuando se utilizó la columna más alta. Después del tiempo de ruptura, las columnas continuaron eliminando cantidades apreciables de colorante e incluso después de 50 horas de funcionamiento, no se saturaron las columnas.

**Palabras clave:** sulfato de quitosano, alginato, columna de lecho fijo, aumento del pH, Colorante Rojo 40.

## 1 Introduction

Water pollution caused by factories discharging large volumes of wastewater containing colorants (textiles, food, paper, plastics, among others) is a significant problem (Crini & Badot, 2008; Torres-Segundo *et al.*, 2019; Márquez-Rámirez & Michtchenko, 2019). Even though these effluents contain small amounts of dye (less than 10 mg/L), they cause water coloring (No & Meyers, 2005). Because of the ecological problem produced by these pollutants, the treatment of the

generated wastewaters is necessary. One option for the treatment is to use activated carbon which is a quite efficient adsorbent; however, its use in water treatment is not usual because of its high cost, that is why other effective and lower cost adsorbents are sought (Bhatnagar & Sillanpää, 2009). Low-cost adsorbents include alginate and chitosan biopolymers. Alginate is a low-cost biopolymer that has been used to remove basic dyes from water (Jeon *et al.*, 2008). Chitosan (Ch) is a chitin derivative that removes acid dyes from water (Crini & Badot, 2008; Dotto *et al.*, 2012; López-Cervantes *et al.*, 2018; Piccin *et al.*, 2011).

\* Corresponding author. E-mail: lalomendizabal@hotmail.com

Tel. 52 3338396660

<https://doi.org/10.24275/rmiq/IA1123>

issn-e: 2395-8472

It has been reported that alginate-chitosan hydrogels have been used for the treatment of wastewater containing metal ions or dyes (Qin *et al.*, 2007; Verduzco-Navarro *et al.*, 2016; Gotoh *et al.*, 2004; Vijaya *et al.*, 2008; Ríos-Donato *et al.*, 2018; Pérez-Escobedo, *et al.*, 2016).

However, Ch shows solubility if the pH is less than 6.0, which prevents its use for the removal of dyes from aqueous solutions with acidic pH (Rinaudo, 2006). Therefore, to be able to use the Ch at low pH, it has been reported that it has been chemically modified (e.g. crosslinking, grafting or sulfation) (Flores-Alamo *et al.*, 2015; Jayakumar *et al.*, 2007; Kyzas & Bikiaris, 2015; Zhou *et al.*, 2014). One of the modifications of Ch that allows its use in acid pH is its partial sulfation (ChS). This ChS has been used to remove dyes or metal ions from acidic aqueous solutions in batch systems (Ríos-Donato *et al.*, 2013; Ríos-Donato *et al.*, 2017; Verduzco-Navarro *et al.*, 2016; Balleño *et al.*, 2016).

Nevertheless, despite the high number of reports of adsorption for dyes using chitosan in batch studies, it is difficult to establish clear trends in their ability to adsorb dyes due to the variability of published results. One of the main factors affecting this variability is that most batch experiments have not taken into account the change in pH of the solution when it comes into contact with Ch (Crini & Badot, 2008; Rinaudo, 2006). Only in a few studies, the pH change of the dye solution during the adsorption process has been mentioned. For example, for the removal of Acid Green 25 from aqueous solution using Ch, Gibbs *et al.* (2003), reported that the use of Ch as an adsorbent caused the pH of the solution to increase.

Sakkayawong *et al.* (2005) reported for the adsorption of Reactive Red (RR141) by Ch, that the initial pH of the dye solutions (2.0-5.0) increased to 8.0-8.5 at the end of the batch experiments. Some strategies have been used to keep the pH constant; Gibbs *et al.* (2003) maintained the pH of the solution constant by the micro addition of 1 M sulphuric acid or 1 M sodium hydroxide, or alternatively by doing pre-conditioning of the Ch by immersing it in a sulphuric acid solution at a pH of 3.0 previously to the adsorption process. Chatterjee *et al.* (2005) proposed the conditioning of the chitosan beads with ammonium sulfate to reduce the pH sensitivity of the process. The pH can also be kept constant using a buffer solution (Chiou *et al.*, 2004; Piccin *et al.*, 2011). These strategies are useful for adsorption in batch systems. However, the removal of contaminants from water by batch processes is limited to small

volumes of effluent, while fixed-bed column systems offer high removal efficiency for large volumes of contaminated water (Aksu, Çağatay, & Gönen, 2007; López-Cervantes *et al.*, 2018; Patel, 2019). In a batch system, the concentration of the dye decreases with time; however, at the end of the process, it cannot be lower than that of the equilibrium. In a fixed-bed column system, the concentration of the dye entering the column is constant, so the concentration gradient is maximized at all times, resulting in that for a long time the concentration of the dye in the effluent may be zero or very small (purification period) and with that a higher removal capacity of the solute is obtained (Acheampong *et al.*, 2012; Cussler, 2009; McKay, 2007; Patel, 2019).

In this work, the ChS was dispersed into calcium alginate hydrogel beads (Alg-ChS), and the beads were used to pack the glass columns. The packed columns were used to remove Red Dye 40 from aqueous acidic solutions. The effect of initial dye concentration, flow rate, and the increase in pH of the dye solution at the exit of the column on the efficiency of the columns is reported. To the best of our knowledge, the use of Alg-ChS beads to remove the Red Dye 40 using fixed-bed columns, and the modification of the pH of the dye solution as it passes through the column has not yet been reported in the literature.

## 2 Materials and methods

### 2.1 Materials

Chitosan food grade (Ch) with a degree of deacetylation of 90% was from América Alimentos S.A. de C.V (Mexico). Acetic acid (Fermont, Mexico), Dimethylformamide (Flucka, USA), Chlorosulfonic acid (Sigma-Aldrich, USA) and methanol (Fermont, Mexico) were used as received. Chitosan sulfate (ChS) (Figure 1) was synthesized following the procedure reported by Ríos Donato *et al.* (2017).

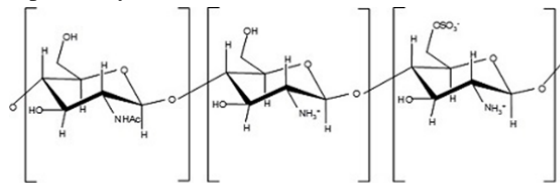


Fig. 1. Structure of the chitosan sulfate.

## 2.2 Methods

### 2.2.1 Preparation and characterization of the Alg-ChS beads

Since ChS was obtained in powder form, it could not be used to pack the columns, because it would cause a high drop in hydrodynamic pressure or obstruction of the column (Vieira *et al.*, 2014), then the ChS was dispersed into calcium alginate hydrogel beads (Alg-ChS) and used to fill the columns. In a flask, an aqueous solution of sodium alginate (1.5% w/w) was mixed with ChS powder (diameter less than 75 microns) under constant agitation to obtain a suspension. The flask was connected to the encapsulating equipment, and the beads were obtained by passing the suspension through a 1000  $\mu\text{m}$  diameter nozzle at a pressure of 250 mBar and a frequency of 600 Hz. The beads were collected in a 0.1 M aqueous solution of  $\text{CaCl}_2$  and left there for 6 hours. Then, the beads were washed, immersed in bidistilled water and stored under refrigeration.

The morphology and surface area of the Alg-ChS beads were observed in a Hitachi TM 1000 scanning electron microscope. The average diameter of the beads was determined by measuring 100 beads using a Veriko Digital Neiko caliper. The concentration of ChS in the Alg-ChS hydrogels was determined by gravimetry following the procedure reported by Verduzco-Navarro *et al.* (2016), and the concentration of calcium alginate was determined using the methodology described by Rfios-Donato *et al.* (2018).

### 2.2.2 Adsorption equilibrium

Aqueous solutions with different concentrations of Red Dye 40 (Figure 2) were prepared. The molecular structure of Red Dye 40 is shown in Figure 2.

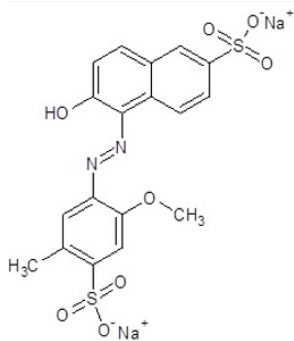


Fig. 2. Red Dye 40 chemical structure.

The pH was adjusted to 5.0 using solutions of 0.1 M HCl. A volume of 10 mL of the dye solution and 1.74 g of Alg-ChS hydrogel beads, was added to a 15 mL centrifuge vial. Then the tubes were placed in a Thermoshaker (MCR, AccesoLab) at 25 °C under continuous agitation (75 RPM) until equilibrium was reached (24 h). The solution was separated by decantation, the pH was measured, and the amount of dye remaining was determined by UV-visible spectrophotometry at the wavelength of 500 nm. The amount of dye adsorbed by unit of weight ( $q_e$ ) was calculated with equation 1.

$$q_e = \frac{(C_0 - C_e)V}{m} \quad (1)$$

where  $m$  is the mass of ChS,  $C_0$  is the initial concentration of the dye,  $C_e$  is the concentration at equilibrium, and  $V$  is the volume of the dye solution. Each run was carried out by triplicate, and the average value is reported. The data obtained from the isotherms at equilibrium were adjusted to the Langmuir model (equation 2) (Crini & Badot, 2008):

$$\frac{C_e}{q_e} = \frac{C_e}{q_m} + \frac{1}{q_m K_L} \quad (2)$$

where  $q_m$  is the maximum adsorption capacity (mg/g) and  $K_L$  is the Langmuir constant (L/mg).  $q_e$  and  $C_e$  are determined from the slope and intercept of the straight line obtained by plotting ( $C_e/q_e$ ) vs.  $C_e$ . The Freundlich model (equation 3) (Crini & Badot, 2008) was also used to fit the data:

$$\log q_e = \log K_F + \frac{1}{n} \log C_e \quad (3)$$

where the Freundlich constant  $K_F$  is an adjustment parameter and  $1/n$  is the intensity of the adsorption interaction (Dada *et al.*, 2012).

### 2.2.3 Fixed-bed columns

For the dye removal two glass columns with an internal diameter of 1.8 cm and bed height of 13 or 33 cm, filled with 18 and 45 g of Alg-ChS hydrogel beads respectively, were used. A dye solution with a predetermined concentration and a pH 5.0 was fed through the bottom of the column with the desired flow rate using a peristaltic pump. Samples were taken at the exit of the column at different time intervals, and its concentration was measured using a visible light spectrophotometer (UNICO Model 1000) at a wavelength of 500 nm. First, calibration curves of Red 40 solutions at different pH's and at the wavelength of

500 nm were obtained. The adsorption capacity ( $q_i$ ) of the column at time  $i$  was determined with equation (4):

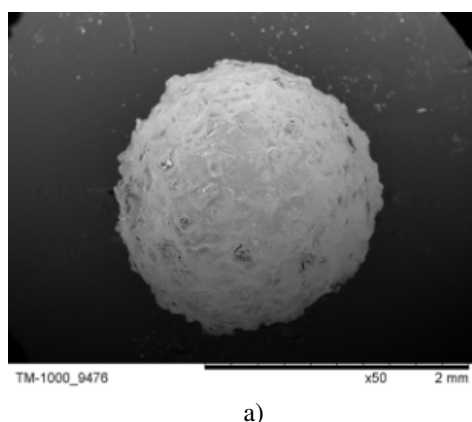
$$q_i = \frac{QC_0 \int_{t=0}^{t=t_i} \left(1 - \frac{C_i}{C_0}\right) dt}{m} \quad (4)$$

where  $m$  corresponds to the mass of adsorbent,  $Q$  to the flow rate,  $C_0$  is the concentration of Red Dye 40 at the entrance of the column,  $C_i$  is the concentration of Red Dye 40 at the exit of the column and  $t$  represents the time.

### 3 Results and discussion

#### 3.1 Beads characterization

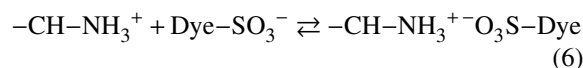
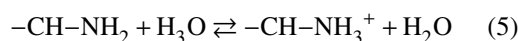
The Alg-ChS hydrogel beads had quasi-spherical shape with an irregular surface and an average diameter of  $2.09 \pm 0.24$  mm (Figure 3a); the ChS particles immersed in the bead can be observed in the amplified image (Figure 3b). Gravimetric analysis showed that the hydrogels contained by weight 3.0% alginate, 0.7% ChS and 96.3% water. The obtained percentage of ChS in the beads was limited by interaction of the protonated amine groups of ChS with their sulfate groups (Agulló *et al.*, 2004) and with the alginate carboxylate groups, causing ChS agglomeration (Qin *et al.*, 2007). If the percentage of ChS increased, larger agglomerates formed that obstructed the nozzle of the encapsulator equipment. By potentiometric titration, it was found that the ChS contains 83.2% of protonatable amino groups and that its  $pK_a$ 's values were 5.67 and 8.0.



#### 3.2 Adsorption equilibrium

Dye adsorption batch experiments were carried out at 25 °C. Table 1, shows the initial pH, the initial dye concentration ( $C_0$ ), the binding capacity of ChS at equilibrium ( $q_e$ ), the dye concentration at equilibrium ( $C_e$ ), and the final pH. In this Table, it can be observed that the pH at the end of the experiments was much higher (5.9-6.8) than the initial one (5.0). The increase in pH can be explained by proton transfer from the solution to the amino and carboxylate groups (Fourest *et al.*, 1996). An important factor in the adsorption mechanism is the pH as it affects the surface of the adsorbent and the degree of ionization of the material in the dissolution (Igberase, Osifo, & Ofomaja, 2014).

The following reactions show the protonation of the amino groups that cause the increase in the pH of the solution, and the mechanism of dye adsorption by the amino groups:



where  $-\text{CH}$  represents the surface of the ChS, and  $\text{O}_3\text{S}-\text{Dye}^-$  the Red Dye 40.

Table 1 shows that the initial concentration of the dye also affects the pH of the final solution due to that some of dye is being protonated (Fourest & Volesky, 1996).

Because alginate does not adsorb acid dyes, the Red Dye 40 was removed only by ChS. It has been reported that alginate hydrogels did not remove the acid dye methyl orange from water solutions (Jeon *et al.*, 2008).

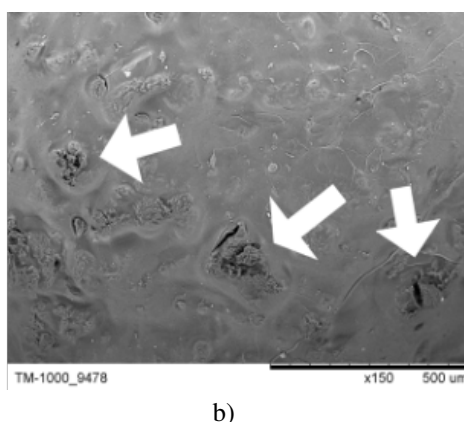


Fig. 3. SEM micrographs of an Alg-ChS hydrogel bead: a) 50x. b) 150x.

Table 1. Red Dye 40 adsorption onto Alg-ChS at equilibrium at 25 °C and initial pH = 5.0.

$C_0$ (mg/L)	$C_e$ (mg/L)	$q_e$ (mg/g SQ)	pH <sub>e</sub>
20	0	14.5	5.9
98	0.26	70.3	6.2
200	7.72	138.4	6.6
225	17.13	149.3	6.6
235	20	154.5	6.7
300	45.6	182.8	6.8
390	110.1	199.8	6.8
490	178	224.1	6.8

Table 2. Isotherm constants of the Langmuir and Freundlich models for adsorption of Red Dye 40.

Langmuir			Freundlich		
$q_m$ (mg/g)	$K_L$ (L/mg)	$R^2$	$K_F$ (mg <sup>1-1/n</sup> L <sup>1/n</sup> /g)	$n$	$R^2$
227	0.139	0.994	91.2	5.7	0.992

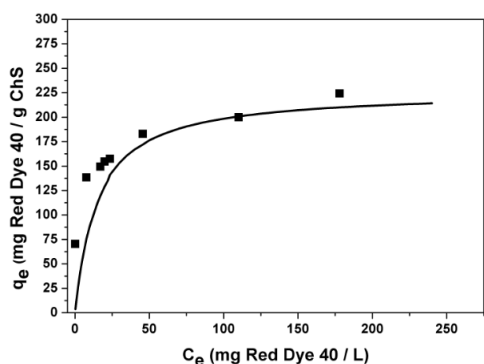


Fig. 4. Adsorption equilibria of Red Dye 40 at 25 °C and initial pH = 5.0.

Verduzco-Navarro *et al.* (2016) reported that there was negligible sorption of the acid Red Dye 40 in batch experiments using alginate hydrogel beads. The experimental equilibrium adsorption data (Table 1) were adjusted using Langmuir and Freundlich's models. By fitting the equilibrium data with the Langmuir model, a straight line was obtained with

a correlation coefficient of 0.9942, and with the Freundlich model, the correlation coefficient of the straight line was 0.9927. Then, the adsorption isotherm was described more precisely with the Langmuir model. Table 2 shows the isothermal constants of the Langmuir and Freundlich models.

Figure 4 shows that the amount of dye adsorbed by ChS at equilibrium ( $q_e$ ) increases with increasing initial dye concentration ( $C_0$ ) and levels off around  $q_e = 230$  mg/g, and that the Langmuir model fits the experimental data closely.

### 3.3 Columns' behavior

In Table 3, for the adsorption of Red Dye 40 using columns packed with Alg-ChS hydrogel, the following results are reported: breakthrough time ( $t_b$ ), the adsorbed dye by the ChS (mg/g of ChS) at the breakthrough time ( $q_b$ ), at 50 hours ( $q_{50}$ ) and at 450 hours ( $q_{450}$ ). When the concentration at the exit of the column was 10% of the concentration of the incoming solution, it was considered that the breakthrough time ( $t_b$ ) had been reached.

Table 3. Adsorption of Red Dye 40 by columns packed with Alg-ChS hydrogel.

Test	1	2	3	4
pH <sub>input</sub>	5	5	5	5
$C_0$ (mg/L)	20	20	20	20
Flow rate (mL/h)	20	40	20	40
Column height (cm)	33	33	13	13
mhydrogel (g)	45	45	18	18
$t_b$ (h)	1.8	0.5	0.3	0.1
$q_b$ (mg/g ChS)	2.24	1.14	0.92	0.42
$q_{50}$ (mg/g ChS)	31.6	23.4	25.6	14.7
$q_{450}$ (mg/g ChS)	128		129	

### 3.4 Flow effect

Aqueous solutions of Red Dye 40 at pH 5.0 and concentration of 20 mg/L were fed to the 13 and 33 cm height columns packed with 18 g and 45 g of Alg-ChS hydrogel beads respectively. Adsorption tests were performed using flow rates of 20 and 40 mL/h. Table 3 shows that the breakthrough time decreases approximately three times as much when the flow rate is increased to 40 mL/h and that the amount of adsorbed dye ( $q_b$  and  $q_{50}$ ) also decreases. These results can be explained because although there is more colorant that pass through the column in each time the residence time of the solution in the column is reduced; in that way, the dye has less opportunity to interact with the adsorbent (Súarez *et al.*, 2019).

Figure 5 shows that when the flow decreases, the breakthrough curves shifted to longer times and become less steep. These behaviors can be explained by the lower amount of dye passing through the column at any given time, leading to lower mass transfer rate (Futalan *et al.*, 2011; López-Cervantes *et al.*, 2018; Zou *et al.*, 2013; Suárez-Vazquez *et al.*, 2019). In this Figure, it is not observed the typical sigmoidal curve obtained in adsorption processes using fixed-bed columns, where after the breakthrough time, the outlet concentration increases fast, and in a relatively short time the column saturates (Al-Remawi, 2012; Cussler, 2009). In this work, after the breakthrough time, the concentration of dye at the exit of the column increases rapidly, then it becomes relatively constant for a certain time and then it increases again; when the test was interrupted, the columns had not yet reached saturation which is confirmed by Table 1, because for a value of  $C_e$  of 20 mg/L, the adsorption capacity at equilibrium ( $q_e$ ) is close to 155 mg/g ChS, which is a value higher than that obtained at 450 hours (128-129 mg/g ChS). The slow approach to saturation is due to the dye having to pass through the hydrogel to reach the ChS particles, which makes the mass transfer rate of the dye slow. It has been reported that asymmetric sigmoidal curves with a slow approach to saturation may be due to mass transfer limited by diffusion (Pires-Cruz *et al.*, 2019; Tovar-Gómez *et al.*, 2013). Breakthrough curves obtained with a flow rate of 40 mL/h seem to approach saturation more quickly than curves obtained with a flow rate of 20 mL/h. At a high flow rate, the time for the dye to contact the adsorbent is not sufficient for the system to reach equilibrium before the solution leaves the column (Chakraborty *et al.*, 2013).

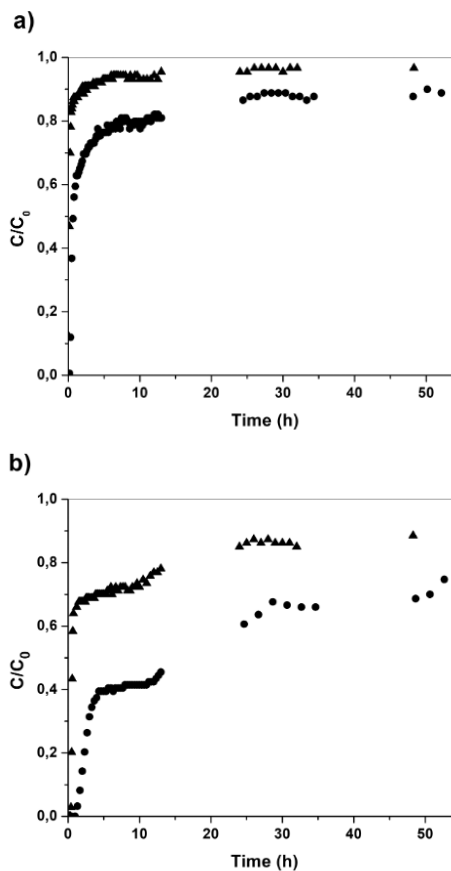


Fig. 5. Breakthrough curves for the Red Dye 40 adsorption onto Alg-ChS beads, dye concentration 20 mg/L, pH= 5.0; flow rate: ● 20 mL/h; ▲ 40 mL/. Column height a) 13 cm; b) 33 cm.

Figure 6 shows that the solution leaves the column at a much higher pH than the incoming solution, and as the dye solution continues to pass through the column, the pH of the output solution decreases. However, even at the end of the experiments the pH value remains much higher than that of the input solution indicating that column saturation has not been reached. The increase in pH is due to the continuous transfer of protons from the solution to the amino and carboxylate groups of the adsorbent. Similar results were obtained in all the experiments. The adsorption of the dye is favored by the pH increase since more amino groups become positively charged (Kyzas *et al.*, 2010) and can interact electrostatically with the sulfonate groups of the dye (Crini & Badot, 2008). Due to the proton transfer from the incoming solution to the amino groups, new active sites are continuously being generated, which can explain the anomalous behavior of the breakthrough curves. Mesquita *et al.*

(2108) reported curves similar to those obtained here in the removal of organic refractory materials using a fixed bed filled with bone char; after the breakthrough time, the output concentration increased rapidly, it then stabilized for a while and then it increased again; this behavior was attributed to the appearance of new active sites.

### 3.5 Effect of column height

Aqueous solutions of Red Dye 40 at pH 5.0 and a concentration of 20 mg/L were fed to 13 and 33 cm high columns filled with Alg-ChS hydrogel beads. Flow rates of 20 and 40 mL/h were used. In Table 3 it can be noticed that by raising the column height the breakthrough time and the values of  $q_b$  and  $q_{50}$  increased because of the larger amount of active groups which are the cause of the removal (Chen *et al.*, 2012; Saadi *et al.*, 2015; Che-Galicia *et al.*, 2014).

In Figure 7 it can be observed that when increasing the length of the column, independently of the flow, the breakthrough time shifts to longer times and the breakthrough curve becomes less steep. It has been reported a similar behavior of breakthrough curves when increasing column length on the adsorption of crystal violet using bone char (Pires-Cruz *et al.*, 2019) and on the adsorption of an azo dye on chitosan impregnated with a cationic surfactant (Rouf & Nagapadma, 2015). Rupture curves obtained with the shortest column appear to approximate saturation more rapidly than those obtained with the higher column due to fewer active sites and more axial dispersion, resulting in insufficient time for the adsorbate to be totally removed (Futalan *et al.*, 2011).

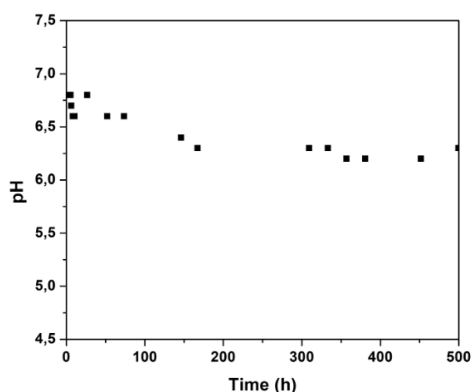


Fig. 6. pH of the output solution as a function of time. Column height of 13 cm, flow rate 20 mL/h, dye concentration 20 mg/L and input solution pH 5.0.

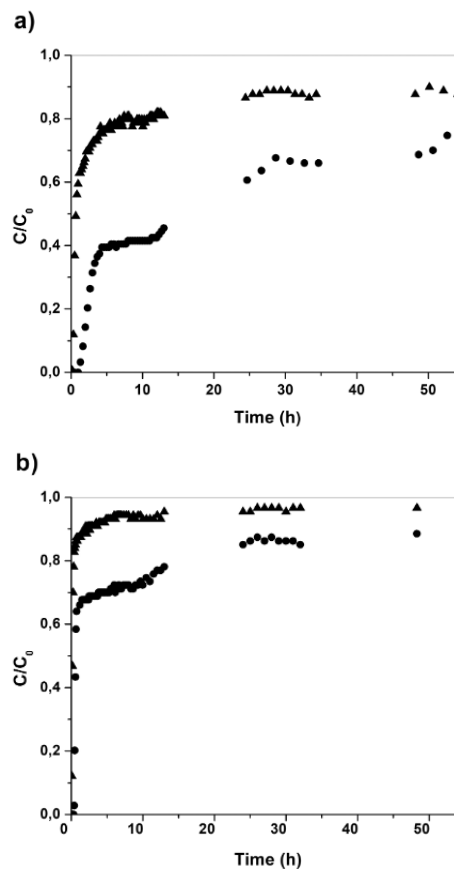


Fig. 7. Breakthrough curves for the Red Dye 40 adsorption onto Alg-ChS beads, dye concentration 20 mg/L, pH 5.0, column height, ● 33 cm; ▲ 13 cm. Flow rate a) 20 mL/h; b) 40 mL/h

## Conclusions

Alg-ChS hydrogels were prepared and used in fixed-bed columns for the removal of Red Dye 40 from acidic aqueous solutions, obtaining good efficiency and high dye removal capacity. The typical sigmoidal curve that is obtained in adsorption processes using fixed-bed columns was not obtained here. After the breakthrough time, the columns continued removing appreciable amounts of dye and even after 450 hours of operation the columns did not reach saturation. The pH of the dye solutions at the exit of the columns was much higher than that of the entry due to the continuous transfer of protons from the aqueous solution to the amino and carboxylate groups; the protonation of these groups was favorable for the removal of the dye. As the flow increased, the amount

of dye removed decreased. Greater dye removal was obtained by increasing the column height. It was concluded that fixed bed columns packed with alginate hydrogels and chitosan sulfate could be used for the removal of Dye Red 40 from acidic aqueous solutions.

### Acknowledgements

This research was supported by a grant from the Consejo Nacional de Ciencia y Tecnología, CONACYT, (CB-2014-1-241108). One author (I.P.V.N) acknowledges the scholarship from CONACyT.

### References

- Acheampong, M., Pakshirajan, K., Annachhatre, A., & Lens, P. N. L. (2012). Removal of Cu(II) by biosorption onto coconut shell in fixed-bed column systems. *Journal of Industrial and Engineering Chemistry* 19. <https://doi.org/10.1016/j.jiec.2012.10.029>
- Agulló, E., Mato, R., Peniche, C., Tapia, C., Heras, A., & San Roman, J. (2004). Quitina y quitosano: obtención, caracterización y aplicaciones. In: *Fuentes y Procesos de Obtención*.
- Aksu, Z., Çağatay, S. S., & Gönen, F. (2007). Continuous fixed bed biosorption of reactive dyes by dried *Rhizopus arrhizus*: Determination of column capacity. *Journal of Hazardous Materials* 143, 362-371. <https://doi.org/10.1016/j.jhazmat.2006.09.039>
- Al-Remawi, M. M. A. (2012). Properties of chitosan nanoparticles formed using sulfate anions as crosslinking bridges. *American Journal of Applied Sciences* 9, 1091-1100.
- Balleño, A., Aranda-García, F., Morales, J. A., Mendizábal, E., & Katime, I. (2016). Hidrogeles de alginate-quitosano y alginate sulfato de quitosano para la remoción de iones cobre. *Revista Iberoamericana de Polímeros* 17, 255-265.
- Bhatnagar, A., & Sillanpää, M. (2009). Applications of chitin- and chitosan-derivatives for the detoxification of water and wastewater - A short review. *Advances in Colloid and Interface Science* 152, 26-38. <https://doi.org/10.1016/j.cis.2009.09.003>
- Chakraborty, S., Chowdhury, S., & Saha, P. Das. (2013). Artificial neural network (ANN) modeling of dynamic adsorption of crystal violet from aqueous solution using citric-acid-modified rice (*Oryza sativa*) straw as adsorbent. *Clean Technologies and Environmental Policy* 15, 255-264. <https://doi.org/10.1007/s10098-012-0503-4>
- Che-Galicia G., Martínez-Vera C., Ruiz-Martínez R. S. and Castillo-Araiza C. O. (2014). Modelado de un adsorbedor de lecho fijo basado en un modelo de isoterma o un modelo cinético aparente. *Revista Mexicana de Ingeniería Química* 13, 539-553. <https://doi.org/10.1111/j.1432-1033.1983.tb07389.x>
- Chen, S., Yue, Q., Gao, B., Li, Q., Xu, X., & Fu, K. (2012). Adsorption of hexavalent chromium from aqueous solution by modified corn stalk: A fixed-bed column study. *Bioresource Technology* 113, 114-120. <https://doi.org/10.1016/j.biortech.2011.11.110>
- Chiou, M.-S., Ho, P. Y., & Li, H. Y. (2004). Adsorption of anionic dyes in acid solutions using chemically cross-linked chitosan beads. *Dyes and Pigments* 60, 69-84. [https://doi.org/10.1016/S0143-7208\(03\)00140-2](https://doi.org/10.1016/S0143-7208(03)00140-2)
- Crini, G., & Badot, P. M. (2008). Application of chitosan, a natural aminopolysaccharide, for dye removal from aqueous solutions by adsorption processes using batch studies: A review of recent literature. *Progress in Polymer Science* 33, 399-447. <https://doi.org/10.1016/j.progpolymsci.2007.11.001>
- Cussler, E. L. (2009). *Adsorption. Diffusion: Mass Transfer in Fluid Systems* (Cambridge Series in Chemical Engineering). Cambridge: Cambridge University Press. (pp. 375-403). <https://doi.org/10.1017/CB09780511805134.015>
- Dada, A. , Olalekan, A., Olatunya, A., & Dada, O. (2012). Langmuir, freundlich temkin and Dubinin-Radushkevich isotherms studies of equilibrium sorption of Zn<sup>2+</sup> unto phosphoric acid modified rice husk. *IOSR Journal of Applied Chemistry* 3, 38-45. <https://doi.org/10.9790/5736-0313845>

- Dotto, G. L., Vieira, M. L. G., & Pinto, L. A. A. (2012). Kinetics and mechanism of tartrazine adsorption onto chitin and chitosan. *Industrial & Engineering Chemistry Research* 51, 6862-6868. <https://doi.org/10.1021/ie2030757>
- Flores-Alamo, N., Solache-Rios, M. J., Gómez-Espinoza, R. M., & García Gaytan, B. (2015). Estudio de adsorción competitiva de cobre y zinc en solución acuosa utilizando Q/PVA/EGDE. *Revista Mexicana de Ingeniería Química* 14, 801-811.
- Fourest, E., & Volesky, B. (1996). Contribution of sulfonate groups and alginate to heavy metal biosorption by the dry biomass of *Sargassum fluitans*. *Environmental Science and Technology* 30, 277-282. <https://doi.org/10.1021/es950315s>
- Futalan, C. M., Kan, C. C., Dalida, M. L., Pascua, C., & Wan, M. W. (2011). Fixed-bed column studies on the removal of copper using chitosan immobilized on bentonite. *Carbohydrate Polymers* 83, 697-704. <https://doi.org/10.1016/j.carbpol.2010.08.043>
- Gotoh, T., Matsushima, K., & Kikuchi, K. I. (2004). Preparation of alginate-chitosan hybrid gel beads and adsorption of divalent metal ions. *Chemosphere* 55, 135-140. <https://doi.org/10.1016/j.chemosphere.2003.11.016>
- Igberase, E., Osifo, P., & Ofomaja, A. (2014). The adsorption of copper (II) ions by polyaniline graft chitosan beads from aqueous solution: Equilibrium, kinetic and desorption studies. *Journal of Environmental Chemical Engineering* 2, 362-369. <https://doi.org/10.1016/j.jece.2014.01.008>
- Jayakumar, R., Nwe, N., Tokura, S., & Tamura, H. (2007). Sulfated chitin and chitosan as novel biomaterials. *International Journal of Biological Macromolecules* 40, 175-181. <https://doi.org/10.1016/j.ijbiomac.2006.06.021>
- Jeon, Y. S., Lei, J., & Kim, J. H. (2008). Dye adsorption characteristics of alginate/polyaspartate hydrogels. *Journal of Industrial and Engineering Chemistry* 14, 726-731. <https://doi.org/10.1016/j.jiec.2008.07.007>
- Kyzas, G. Z., & Bikiaris, D. N. (2015). Recent modifications of chitosan for adsorption applications: A critical and systematic review. *Marine Drugs* 13. <https://doi.org/10.3390/md13010312>
- Kyzas, G. Z., Kostoglou, M., & Lazaridis, N. K. (2010). Relating interactions of dye molecules with chitosan to adsorption kinetic data. *Langmuir* 26, 9617-9626. <https://doi.org/10.1021/la100206y>
- López-Cervantes, J., Sánchez-Machado, D. I., Sánchez-Duarte, R. G., & Correa-Murrieta, M. A. (2018). Study of a fixed-bed column in the adsorption of an azo dye from an aqueous medium using a chitosan-glutaraldehyde biosorbent. *Adsorption Science and Technology* 36, 215-232. <https://doi.org/10.1177/0263617416688021>
- Mahmoodi, N. M. (2011). Equilibrium, kinetics, and thermodynamics of dye removal using alginate in binary systems. *Journal of Chemical and Engineering Data* 56, 2802-2811. <https://doi.org/10.1021/je101276x>
- Márquez-Rámirez E., Michtchenko A., Zacahua-Tlacuatl G. (2019). Effects of radiation of CO<sub>2</sub> laser on natural dolomite for the degradation of azo dye reactive black 5 by photocatalysis. *Revista Mexicana de Ingeniería Química* 18, 555-569.
- McKay, G. (2007). Design models for adsorption systems in wastewater treatment. *Journal of Chemical Technology and Biotechnology* 31, 717-731. <https://doi.org/10.1002/jctb.503310197>
- No, H. K., & Meyers, S. P. (2005). *Handbook of Carbohydrate Engineering*. Cap. 19. Treatment of wastewaters with the biopolymer chitosan.
- Patel, H. (2019). Fixed-bed column adsorption study: a comprehensive review. *Applied Water Science* 9, 1-17. <https://doi.org/10.1007/s13201-019-0927-7>
- Pérez-Escobedo, A., Díaz-Flores, P.E., Rangel-Méndez, J. R., Cerino-Cordova F. J., Ovando-Medina, V.M., Alcalá-Jáuregui, J. A. (2016).

- Fluoride adsorption capacity of composites based on chitosan- zeolite-algae. *Revista Mexicana de Ingeniería Química* 15, 139-147
- Piccin, J. S., Dotto, G. L., Vieira, M. L. G., & Pinto, L. A. A. (2011). Kinetics and mechanism of the food dye FD&C Red 40 adsorption onto chitosan. *Journal of Chemical and Engineering Data* 56, 3759-3765. <https://doi.org/10.1021/jc200388s>
- Pires-Cruz, M. A., Matos-Guimarães, L. C., Ferreira da Costa Júnior, E., Ferreira Rocha, S. D., & da Luz Mesquita, P. (2019). Adsorption of crystal violet from aqueous solution in continuous flow system using bone char. *Chemical Engineering Communications* 0, 1-10. <https://doi.org/10.1080/00986445.2019.1596899>
- Qin, Y. M., Cai, L. L., Feng, D.M., Shi, B.B., Liu, J. J., Zhang, W. T., Shen, Y. C. (2007). Combined use of chitosan and alginate in the treatment of wastewater. *Journal of Applied Polymer Science* 104, 3581-3587. <https://doi.org/10.1002/app.26006>
- Rinaudo, M. (2006). Chitin and chitosan: Properties and applications. *Progress in Polymer Science* 31, 603-632. <https://doi.org/10.1016/j.progpolymsci.2006.06.001>
- Ríos-Donato, N., Marmolejo-Carranza, R., Blanco-Aquino, A., García-Gaytán, B., & Mendizabal, E. (2013). Eliminación de colorantes de disoluciones acuosas utilizando sulfato de quitosano. *Revista Iberoamericana de Polímeros* 14, 257-263.
- Rios-Donato, N., Peña-Flores, A. M., Katime, I., Leyva-Ramos, R., & Mendizabal, E. (2017). Kinetics and thermodynamics of adsorption of red dye 40 from acidic aqueous solutions onto a novel chitosan sulfate. *Afinidad* 74, 214-220.
- Ríos Donato, N., Carrión Espinoza, L. G., Mayorga Rivera, J. A., Verduzco Navarro, I. P., Katime, I., & Mendizabal, E. (2018). Removal of Cd ( II ) from aqueous solutions by batch and continuous process using chitosan sulfate dispersed in a calcium alginate hydrogel. *Afinidad* 75, 112-118.
- Rouf, S., & Nagapadma, M. (2015). Modeling of fixed bed column studies for adsorption of azo dye on chitosan impregnated with a cationic surfactant. 6, 538-545.
- Saadi, Z., Saadi, R., & Fazaeli, R. (2015). Dynamics of Pb(II) adsorption on nanostructured  $\gamma$ -alumina: Calculations of axial dispersion and overall mass transfer coefficients In the fixed-bed column. *Journal of Water and Health* 13, 790-800. <https://doi.org/10.2166/wh.2015.271>
- Suárez-Vazquez, S. I., Vidales-Contreras, J. A., Márquez-Reyes, J., Cruz-López, A., & García-Gómez, C. (2019). Remoción del colorante rojo congo usando hidroxido metálico electrocoagulado en una columna de lecho fijo: caracterización, optimización y estudios de modelado. *Revista Mexicana de Ingeniería Química* 18, 1133-1142.
- Torres-Segundo, C., Vergara-Sánchez, S., Reyes-Romero, P., Gómez-Díaz, A., Cruz-López, J., & García-Gómez, C. (2019). Effect on discoloration by nonthermal plasma in dissolved textile dyes:acid Black 194. *Revista Mexicana de Ingeniería Química* 18, 939-947.
- Tovar-Gómez, R., Moreno-Virgen, M. R., Dena-Aguilar, J. A., Hernández-Montoya, V., Bonilla-Petriciolet, A., & Montes-Morán, M. A. (2013). Modeling of fixed-bed adsorption of fluoride on bone char using a hybrid neural network approach. *Chemical Engineering Journal* 228, 1098-1109. <https://doi.org/10.1016/j.cej.2013.05.080>
- Verduzco-Navarro, I. P., Ríos-Donato, N., Mendizabal, E., & Katime, I. (2016). Remoción de colorante Rojo 40 mediante de perlas de alginato-quitosana y alginato- sulfato de quitosana. *Revista de Ciencias Ambientales y Recursos Naturales* 2, 33-43.
- Vijaya, Y., Popuri, S. R., Boddu, V. M., & Krishnaiah, A. (2008). Modified chitosan and calcium alginate biopolymer sorbents for removal of nickel (II) through adsorption. *Carbohydrate Polymers* 72, 261-271. <https://doi.org/10.1016/j.carbpol.2007.08.010>
- Zhou, Z., Lin, S., Yue, T., & Lee, T.-C. (2014). Adsorption of food dyes from aqueous solution by glutaraldehyde cross-linked magnetic chitosan nanoparticles. *Journal of Food Engineering* 126, 133-141. <https://doi.org/10.1016/j.jfoodeng.2013.11.014>

Zou, W., Zhao, L., & Zhu, L. (2013). Adsorption of uranium(VI) by grapefruit peel in a fixed-bed column: experiments and prediction of breakthrough curves. *Journal*

*of Radioanalytical and Nuclear Chemistry* 295, 717-727. <https://doi.org/10.1007/s10967-012-1950-4>